Available online at www.sciencedirect.com
ScienceDirect
Biochimica et Biophysica Acta 1778 (2008) 229–241
Biochimica et Biophysica Acta
BBA
www.elsevier.com/locate/bbamem

Amphipathic α-helical peptide, HP (2–20), and its analogues derived from *Helicobacter pylori*: Pore formation mechanism in various lipid compositions

Seong-Cheol Park [a,b,1,2], Mi-Hyun Kim [a,2], Mohammed Akhter Hossain [c], Song Yub Shin [a,d], Yangmee Kim [e], Lorenzo Stella [f], John D. Wade [c], Yoonkyung Park [a,g,*], Kyung-Soo Hahm [a,d,*]

[a] *Research Center for Proteineous Materials (RCPM), Chosun University, Gwangju, Korea*
[b] *Division of Applied Life Sciences (BK21 program), Gyeongsang National University, Jinju, 660-701, Korea*
[c] *Howard Florey Institute, University of Melbourne, Victoria, Australia*
[d] *Department of Cellular·Molecular Medicine School of Medicine, Chosun University, Gwangju, Korea*
[e] *Department of Bioscience and Biotechnology, Konkuk University, Seoul 143-701, Korea*
[f] *Dipartimento di Scienze e Tecnologie Chimiche, Università di Roma, Italy*
[g] *Department of Biotechnology and BK21 Research Team for Protein Activity Control, Chosun University, Gwangju, Korea*

Received 20 March 2007; received in revised form 22 September 2007; accepted 25 September 2007
Available online 2 October 2007

Abstract

In a previous study, we determined that HP(2–20) (residues 2–20 of parental HP derived from the N-terminus of *Helicobacter pylori* Ribosomal Protein L1) and its analogue, HPA3, exhibit broad-spectrum antimicrobial activity. The primary objective of the present study was to gain insight into the relevant mechanisms of action using analogues of HP(2–20) together with model liposomes of various lipid compositions and electron microscopy. We determined that these analogues, HPA3 and HPA3NT3, exert potent antibacterial effects in low-salt buffer and antifungal activity against chitin-containing fungi, while having little or no hemolytic activity or cytotoxicity against mammalian cell lines. Our examination of the interaction of HP(2–20) and its analogues with liposomes showed that the peptides disturb both neutral and negatively-charged membranes, as demonstrated by the release of encapsulated fluorescent markers. The release of fluorescent markers induced by HP(2–20) and its analogues was inversely related to marker size. The pore created by HP(2–20) shows that the radius is approximately 1.8 nm, whereas HPA3, HPA3NT3, and melittin have apparent radii between 3.3 and 4.8 nm. Finally, as shown by electron microscopy, the liposomes and various microbial cells treated with HPA3 and HPA3NT3 showed oligomerization and blebbing similar to that seen with melittin, while HP(2–20) exhibited flabbiness. These results suggest that HP(2–20) may exert its antibiotic effects through a small pore (about 1.8 nm), whereas HPA3 and HPA3NT3 formed pores of a size consistent with those formed by melittin.

Keywords: HP(2–20); Mechanism of action; Fluorescent markers; Oligomerization; Pore-forming

1. Introduction

Membrane-active peptides, including a host of antimicrobials and toxins, have been shown to induce the formation of transmembrane pores. Although the molecular mechanisms by which pore formations occur remain to be thoroughly elucidated, the three mechanisms thus far proposed include the "barrel-stave", "carpet", and "toroidal" models. In the barrel-stave model, peptide helices form a bundle with a central lumen within the membrane, appearing similar to a barrel in which the helical peptides function as the staves [1–5]. This variety of trans-

Abbreviations: BS^3, Bis(sulfosuccinimidyl)suberate; CH, cholesterol; CL, cardiolipin; DCC, dicyclohexylcarbodiimide; Dis-C_3-5, 3,3′, diethylthio-dicarbocyanine iodide; FITC-D, fluorescein isothiocyanate dextrans; HOBT, 1-hydroxy benzotriazole; LPS, lipopolysaccharide; NMP, N-methyl-2-pyrrolidone; PC, egg yolk L-α-phosphatidylcholine; PE, L-α-phosphatidylethanolamine; PG, L-α-phosphatidyl-DL-glycerol; PS, Phosphatidylserine; SM, Sphingomyelin

* Corresponding authors. Research Center for Proteineous Materials (RCPM), Chosun University, Gwangju, Korea. Tel.: +82 62 230 7556; fax: +82 62 227 8345.
E-mail addresses: y_k_park@chosun.ac.kr (Y. Park), kshahm@chosun.ac.kr (K.-S. Hahm).

[1] S-C Park was supported by scholarships in 2007 from the Brain Korea21 project in Korea.
[2] These authors contributed equally to this work.

0005-2736/$ - see front matter © 2007 Elsevier B.V. All rights reserved.
doi:10.1016/j.bbamem.2007.09.020

membrane pore is induced by treatment with compounds such as alamethicin. It was reported that alamethicin produced pores of ~1.8 nm and ~4.0 nm (inner and outer diameter, respectively) at the threshold concentration of the peptide/lipid ratio [6,7]. These dimensions imply that the walls of the channel are ~1.1 nm in thickness, while is similar to the diameter of the alamethicin helix. Thus, its pores are consistent with an arrangement of eight alamethicin monomers in a barrel-stave configuration [1,8,9].

The carpet model elucidates the activity of antimicrobial peptides such as ovispirin [10]. In this case, peptides accumulate on the bilayer surface, oriented in parallel – i.e., in-plane – with the membrane surface [11,12]. The peptides are electrostatically attracted to the anionic phospholipid head groups at numerous sites, and thereby cover the surface of the membrane in a carpet-like manner [13–17].

In the toroidal-pore model, which has been advanced to explain the activity of the magainins [18], protegrins [19], and melittin [1], the polar faces of the peptides associate with the polar head groups of the lipids and remain in this orientation even when they are perpendicularly inserted into the lipid bilayer, a feature which distinguishes it from the barrel-stave model. The magainin-induced toroidal pores are larger and vary in size to a greater extent than has been observed with the alamethicin-induced pores [1]. They evidence an inner diameter of 3.0–5.0 nm and an outer diameter of ~ 7.0–8.4 nm, and each of the pores is thought to harbor 4–7 magainin monomers and ~90 lipid molecules [1,20]. Melittin, magainin, and alamethicin are the prototype peptides employed in studies of the mechanisms underlying pore formation in both the toroidal and barrel-stave models [21].

Stomach mucosa that is infected with *Helicobacter pylori*, the bacterial pathogen associated with gastritis and peptic ulcers, typically shows massive infiltration of inflammatory cells and tissue destruction [22]. Persistence of *H. pylori* in the mucosa has been suggested to be facilitated by *H. pylori*-produced cecropin-like peptides with antibacterial properties. Although *H. pylori* itself is resistant to this peptide, the release of these peptides gives a competitive advantage over other microorganisms [23].

The linear antimicrobial peptide, HP(2–20), is a cationic α-helical peptide that has been isolated from the N-terminal region of the *Helicobacter pylori* ribosomal protein, L1 [24]. This peptide possesses several important functional characteristics; it is bactericidal, it is a neutrophil chemoattractant, and it activates phagocyte NADPH oxidase to produce reactive oxygen species [24].

The primary objective of the present study was to characterize the effects of HP(2–20) and its analogues on a variety of lipid compositions and cell wall components, and to make observations via electron microscopy. In addition, we assessed pore sizes in these zwitterionic vesicles via dextran leakage and transmission electron microscopy.

2. Materials and methods

2.1. Materials

Proteinase K, trypsin, chitin, cellulose, chitosan, curdlan, peptidoglycan (from *Staphylococcus aureus*), LPS (lipopolysaccharide)[1] (from *Escherichia coli* 0111:B4), BCA protein reagent, BS[3] (Bis(sulfosuccinimidyl)suberate), PE (L-α-phosphatidylethanolamine) (Type V, from *E. coli*), SM (sphingomyelin, from bovine brain), CH (cholesterol, from porcine liver), and FITC-D (fluorescein isothiocyanate dextrans), with average molecular masses of 4, 10, 20, 40, 70, and 500 kDa were all purchased from the Sigma Chemical Co. (St. Louis, MO). PG (L-α-phosphatidyl-DL-glycerol), PC (egg yolk L-α-phosphatidylcholine), PS (phosphatidylserine, from brain) and CL (cardiolipin, from *E. coli*) were obtained from Avanti Polar Lipids (Alabaster, AL). $DiSC_3$-5 (3,3′-diethylthio-dicarbocyanine iodide) and calcein were acquired from Molecular Probes (Eugene, OR). All other reagents were of analytical grade. Buffers were prepared in double glass-distilled water.

2.2. Peptide synthesis and purification

All peptides were synthesized via solid-phase methods with Fmoc (N-(9-fluorenyl)methoxycarbonyl)-protected amino acids on an Applied Biosystems Model 433A peptide synthesizer. 4-Methyl benzhydrylamine resin (Novabiochem) (0.55 mmol/g) was employed to create the amidated C-terminus. For each coupling step, the Fmoc-protected amino acid and coupling reagents were added in a 10-fold molar excess with regard to resin concentration. Coupling (60–90 min) was conducted with DCC (dicyclohexylcarbodiimide) and HOBT (1-hydroxy benzotriazole) in NMP (N-methyl-2-pyrrolidone). Cleavage from the resin and the deprotection of the synthesized peptide were conducted using a solution of 90% trifluoroacetic acid, 3% water, 1% triisopropylsilane and 2% each of 1,2-ethanedithiol, thioanisole, and phenol. After repeated ether precipitation, the crude peptide was purified via reversed-phase preparative HPLC on a Waters 15-μm Deltapak C18 column (19×300 mm) using an appropriate 0–60% acetonitrile gradient in 0.1% trifluoroacetic acid. The purity of the purified peptide was then determined via analytical reversed-phase HPLC using a Vydac C18 column (4.6×250 mm, 300 Å, 5 nm). The molecular masses of the peptides were verified with a matrix-assisted laser desorption ionization mass spectrometer (MALDI II, Kratos Analytical Ins.).

2.3. Antimicrobial assay

Candida albicans was cultured at 28 °C in YPD broth. *E. coli* and *S. aureus* were cultured at 37 °C in trypticase soy broth. The antimicrobial activity of each peptide was determined via microdilution assays. In brief, the microorganisms were collected in mid-log phase and suspended in buffer I (low ionic strength buffer; 10 mM sodium phosphate, pH 7.2) or buffer II [high ionic strength buffer; PBS (1.5 mM KH_2PO_4, 2.7 mM KCl, 8.1 mM Na_2HPO_4, 135 mM NaCl, pH 7.2)]. Two-fold serial dilutions of each of the peptides, in a range from 0.39 to 200 μM, in buffers I and II, were arranged in sterile 96-well plates, after which aliquots of the cell suspension (1×10^6 CFU/ml) was added to each well. Plates containing fungal cells were incubated for 2 h at 28 °C, while the plates containing the bacterial cells were incubated at 37 °C for the same amount of time. At the end of the incubation, 50 μl of 20-fold diluted samples were plated on appropriate agar plates, and were then incubated for 24 h, after which the colonies were counted. The lowest concentration of peptide that completely inhibited growth was defined as the MIC. The MIC values were calculated as an average of several independent experiments conducted in triplicate.

2.4. hRBC (human red blood cell) hemolysis

Hemolytic activities were assessed for all peptides, using hRBCs from healthy donors, and collected on heparin. The fresh hRBCs were rinsed three times in PBS via 10 min of centrifugation at 800×*g*, and resuspended in PBS. The peptides dissolved in PBS were then added to 100 μl of the stock hRBCs suspended in PBS (final RBC concentration, 8% v/v). The samples were then incubated with agitation for 60 min at 37 °C, and then centrifuged for 10 min at 800×*g*. The absorbance of the supernatants was assessed at 414 nm; the controls for zero hemolysis (blank) and 100% hemolysis were comprised of hRBCs suspended in PBS and 1% Triton X-100, respectively. Each measurement was conducted in triplicate.

2.5. Cell line and culture

The human keratinocyte HaCaT cell line was obtained from Dr. NE. Fusenig (Heidelberg, Germany). Cells, cultured in 75 cm^2 plastic flasks, were grown in

Dulbecco's modified Eagle medium (DMEM) supplemented with antibiotics (100 U/mL penicillin, 100 μg/mL streptomycin), 10% fetal calf serum, 1 mM pyruvate, and 4 mM L-glutamine. The cells were then cultured at 37 °C in a humidified chamber in an atmosphere containing 5% CO_2.

2.6. Cytotoxicity

The percentage of growth inhibition was evaluated using a MTT (Sigma) assay for the measurement of viable cells. A total of 4×10^3 cells/well was seeded onto a 96-well plate for 24 h, treated with various concentrations of the tested peptides, then incubated for an additional 24 h at 37 °C. Subsequently, 10 μl of MTT at a concentration of 5 mg/ml was added to each of the wells, and the cells were incubated for an additional 4 h. The supernatants were aspirated and 100 μl of DMSO were added to the wells in order to dissolve any remaining precipitate. Absorbance was then measured at a wavelength of 570 nm using an EL_X800 reader (Bio-Tek instruments, Inc., Winooski, VT).

2.7. Peptide binding to microbial cell wall components

In order to determine the *in vitro* binding of synthetic HP-family peptides to curdlan (β-1, 3-glucan), peptidoglycan (β-1, 4-glycosidic linkage between *N*-acetylmuramic acid and *N*-acetylglucosamine), chitin (β-1, 4-*N*-acetyl-D-glucosamine) and cellulose (β-1, 4-glucan), 200 μg of each insoluble polysaccharide was added to 200 μl of buffer I or buffer II containing 5 μg of peptides, then incubated for 1 hour at 20–22 °C with 180 rpm. The mixture was then centrifuged (12,000×*g* for 3 min), and the pellet was washed three times in 0.5 ml of washing buffer (10 mM Tris, pH 7.5, 500 mM NaCl, 0.02% Tween 20). The peptides bound to the insoluble polysaccharides were detached via the addition of SDS-PAGE sample buffer, and then subjected to 16.5% Tricine-SDS-PAGE. LPS binding assays were conducted in essentially the same manner, except that the binding mixture was centrifuged for 15 min at 22,000×*g* at each step in order to precipitate small LPS particles.

2.8. Peptide binding to liposomes

An assay to determine the binding of peptides to various lipids was performed according to the method described by Makino et al. [25], with some modification. In brief, 50 μl of lipid (250 μM) in chloroform was added to each well of a polypropylene microtiter plate (Nunc, Roskilde, Denmark). After evaporation of the solvent at room temperature, the wells were then washed with buffer (10 mM sodium phosphate, pH 7.2) and incubated with 50 μl of 40 μM peptide for 2 h at room temperature. The unbound peptide was removed, and the wells were then washed twice with the same buffer. The concentration of unbound peptide was measured using a BCA kit (Pierce, Rockford, IL) in order to compare the intensities of bound peptide on SDS-PAGE. After washing, Tricine SDS-PAGE buffer was added to each well for the suspension of bound peptide, and the suspensions were subjected to SDS-PAGE on 16.5% Tricine gels. The amount of bound peptide was detected according to the intensity of stained bands as a form of qualitative analysis.

2.9. Calcein release from liposomes

The interaction and permeabilization of peptides against liposomes were assayed by measuring calcein leakage. Calcein-entrapped liposomes were prepared for use in dye leakage experiments as follows. In brief, calcein-entrapped LUVs (large unilamellar vesicles) were prepared by vortexing the dried lipid in dye buffer solution (70 mM calcein, 10 mM HEPES, 150 mM NaCl, 0.1 mM EDTA, pH 7.4). The suspension was freeze–thawed in liquid nitrogen for nine cycles and extruded 30 times through polycarbonate filters (two stacked 0.2-μm pore size filters) using an *Avanti* Mini-Extruder (Avanti Polar Lipids inc., Alabaster, AL). Calcein-entrapped vesicles were separated from free calcein by gel filtration chromatography on a Sephadex G-50 column. Entrapped LUVs in suspensions containing 100 μM lipids were incubated with various concentrations of the peptide (0.6–20 μM). The fluorescence of the released calcein was assessed with a spectrofluorometer (Perkin-Elmer LS55) at an excitation wavelength of 480 nm and an emission wavelength of 520 nm. Complete (100%) release was achieved via the addition of Triton X-100 to a final concentration of 1 mM. Spontaneous leakage was determined to be negligible at this time scale. The experiments were conducted at 25 °C. The apparent percentage of calcein release was calculated in accordance with the following equation [26]

$$\text{Release } (\%) = 100 \times (F - F_0)/(F_t - F_0)$$

in which F and F_t represent the fluorescence intensity prior to and after the addition of the detergent, respectively, and F_0 represents the fluorescence of the intact vesicles.

2.10. Membrane depolarization in bacteria and yeast

Membrane depolarization was assessed using Dis-C_3-5, a lipophilic potentiometric indicator dye.

2.10.1. (i) Gram-positive bacteria

S. aureus was grown to mid-log phase at 37 °C with agitation. The cells were washed once in buffer A (20 mM glucose, 5 mM HEPES, pH 7.3) and resuspended to an OD_{600} of 0.05 in buffer A containing 0.1 M KCl. The cells were then incubated with 1 μM DiS-C_3-5 until stable baseline fluorescence was achieved. The experiments were conducted in sterile 96-well plates at a final volume of 200 μl. The peptides dissolved in buffer A were added in order to achieve the desired concentration, after which membrane depolarization was detected as an increase in the DiS-C_3-5 fluorescence (excitation wavelength, 622 nm; emission wavelength, 670 nm).

2.10.2. (ii) Intact Gram-negative bacteria

The assay for intact Gram-negative bacteria was conducted using exactly the same method as described above, except with *E. coli* ATCC 25922.

2.10.3. (iii) Spheroplasts of Gram-negative bacteria

Spheroplasts of *E. coli* ATCC 25922 bacteria were prepared via an osmotic shocktechnique. First, cells from cultures grown to OD_{600} of 0.8 were harvested via centrifugation, washed twice in buffer C (10 mM Tris/H_2SO_4, 25% sucrose, pH 7.5), and resuspended in buffer C containing 1 mM EDTA. After 10 min of incubation at 20 °C with rotary mixing, the cells were harvested via centrifugation, immediately resuspended in freezing (0 °C) water and incubated for 10 min at 4 °C. The resultant spheroplasts were harvested via centrifugation and resuspended to an OD_{600} of 0.05 in buffer D (20 mM glucose, 5 mM HEPES, 1 M KCl, pH 7.3). Further treatments were conducted as described for *S. aureus*.

2.10.4. (iv) Intact yeast

In order to detect membrane depolarization in intact yeast (*C. albicans*), cells were incubated at 35 °C to mid-log phase in RPMI 1640 (165 mM MOPS, pH 7.0, with L-glutamine and $NaHCO_3$) with agitation and washed with Ca^{2+}- and Mg^{2+}-free PBS, after which the samples (2×10^5 CFU/ml) were incubated with 1 μM DiS-C_3-5 and membrane depolarization was evaluated as described above.

2.11. Preparation of dextran-loaded liposomes and leakage experiments

FITC-labeled dextrans (FD-4, 10, 20, 40, 70 and 500) were utilized as model cytoplasmic components. FD-entrapping liposomes (unilamellar vesicles) with different lipid compositions were prepared using the reverse-phase evaporation method [27], and the concentrations of the FD-entrapped vesicles were determined in triplicate using a phosphorus assay [28]. To prepare FD-entrapped liposomes, a buffer solution (buffer II: PBS) containing 2 mg/ml of the FD was sonicated for 30 min with a lipid solution in chloroform (20 mg/ml) on ice. The chloroform was then gradually removed using a rotary vacuum evaporator at 25 °C, resulting first in the formation of a viscous gel, and then a liposome suspension. Buffer (2 ml) was added, and the suspension was evaporated further for the removal of the remaining solvent. The liposome suspensions were then centrifuged and washed for several cycles at 22,000×g_{av} for 30 min in order to remove unentrapped-FD. The washed liposomes were extruded 30 times through polycarbonate filters (two stacked 0.4-μm pore size filters) using an *Avanti* Mini-Extruder (Avanti Polar Lipids inc., Alabaster, AL) to obtain liposomes of homogeneous size (~400 nm). Aliquots of the peptide solutions at appropriate concentrations were incubated with a suspension of FD-loaded

liposomes (100 μM) for 1–20 min at 25 °C, and were then centrifuged for 30 min at 22,000×*g*. The supernatants were recovered and their leakages were recorded by monitoring the fluorescence intensity of FITC (excitation wavelength: 494 nm, emission wavelength: 520 nm). 100% leakage was achieved upon the addition of Triton X-100 to a final concentration of 1 mM. The percent leakage value was then plotted.

2.12. Cross-linking analysis

HP(2–20) or the indicated analogue was initially incubated for 10 min with PC/cholesterol (10:1, w/w) liposomes at 25 °C, and then for an additional 1 h with 80 μM BS^3. After incubation, the samples were added to tricine sample buffer and subjected to 16.5% Tricine–SDS-PAGE without heating. The peptide bands were identified in the gels after Coomassie Brilliant Blue G-250 staining.

2.13. Transmission electron microscopy (TEM)

Small unilamellar vesicles for TEM analysis were prepared as follows. Dry lipids [PE/PG (7:3, w/w) or PC/cholesterol (10:1, w/w)] were dissolved in chloroform in a small glass vessel. Solvents were removed by nitrogen gas, so that they formed a thin film on the wall of a glass vessel and then lyophilized overnight. Dried thin films were resuspended in 10 mM sodium phosphate buffer by vortex mixing. The lipid dispersions were then sonicated in ice for 10–20 min using a titanium-tip ultrasonicator until the solution became opalescent.

HP and its analogues were incubated with SUVs (small unilamellar vesicles) at 25 °C in 10 mM sodium phosphate buffer. After incubation, the peptides were applied to glow-discharged carbon-coated copper grids for 1 min. The grids were rinsed in the same buffer, and stained with 2% (w/v) uranyl acetate. Electron micrographs were then recorded (FEI Technei 12 microscope) at nominal magnification (×67,000–110,000) with an accelerating voltage of 120 kV.

2.14. Electron microscopic examination of bacterial and fungal membranes

Midgrowth-phase *S. aureus, E. coli*, and *C. albicans* were resuspended at 10^8C.F.U./ml in sodium-phosphate buffer, at a pH of 7.4, supplemented with 100 mM NaCl, and then incubated at 37 °C and 28 °C, respectively, with HP, its analogues, and melittin. Controls were run in the absence of peptide solution. After 30 min, the cells were fixed with an equal volume of 5% (v/v) glutaraldehyde in 0.2 M sodium-cacodylate buffer, at a pH of 7.4. After 2 h of fixation at 4 °C, the samples were filtered on isopore filters (0.2 μm pore size, Millipore, Bedford, MA) and washed extensively with 0.1 M cacodylate buffer, at a pH of 7.4. The filters were then treated with 1% (w/v) osmium tetroxide, washed in 5% (w/v) sucrose in cacodylate buffer, and subsequently dehydrated with a graded series of ethanol. After lyophilization and gold coating, the samples were evaluated on a HITACHI S-2400 instrument (HITACHI, Japan).

2.15. Circular dichroism (CD) analysis in SDS micelles and PC/CH liposome

CD spectra were recorded at 25 °C on a Jasco 810 spectropolarimeter (Jasco, MD, USA) equipped with a temperature control unit. A 0.1-cm path-length quartz cell was used for a 50-μM peptide solution. At least five scans were averaged for each sample and the averaged blank spectra were subtracted. Each spectrum was obtained by averaging five scans in the 250–190 nm wavelength range. All CD spectra are reported in mean residue ellipticity, $[\theta]_{MRW}$, in deg·cm^{2}dmol^{-1}. The α-helical content was determined from the mean residue ellipticities at 222 nm, as indicated in Equation (1) [29].

$$\%\ \text{Helix} = ([\theta]_{obs} \times 100)/\{[\theta]_{helix} \times (1 - 2.57/l)\} \quad (1)$$

where $[\theta]_{obs}$ is the mean-residue ellipticity observed experimentally at 222 nm, $[\theta]_{helix}$ is the ellipticity of a peptide of infinite length with 100% helix population, taken as −39,500 deg·cm^{2}dmol^{-1}, and l is the peptide length or, more precisely, the number of peptide bonds.

3. Results

3.1. Four sets of peptides designed using HP(2–20)

HP(2–20) is a 19-residue amphipathic antimicrobial peptide, with both hydrophilic and hydrophobic faces. In order to correlate antimicrobial activity with the binding to and permeabilization of fungal and bacterial cell membranes, and to determine the mode of action of the peptide, we designed four sets of peptides using HP(2–20) as the parent peptide (Table 1). In order to evaluate the influence of the N- and C-terminal amino acids on the antimicrobial activity and the relationship between the hydrophobic and hydrophilic regions of the peptide, we designed a set of N- and C-terminal-deleted peptides. The importance of hydrophobicity was evaluated using more hydrophobic peptides, in which one or more residues were substituted with Trp. The effect of the addition of positive charges to the peptide was then assessed via the substitution of one or more residues with Lys or Arg. Finally, a fourth type of peptide was designed, which harbored an especially high net charge. The antimicrobial peptide, melittin, functioned as a control.

3.2. Antifungal, antibacterial, hemolytic activities and cell viability of the peptides were assayed

Antifungal activity was assayed against representative pathogenic yeast, which commonly infests immunocompro-

Table 1
Sequence alignment of HP(2–20) and its analogue peptides

Name	Sequence	Net charge
Original source	2 5 10 15 20	
HP (2–20)	AKKVFKRLEKLFSKIQNDK	+5
Truncated peptides		
HPN1(4–20)	KVFKRLEKLFSKIQNDK	+4
HPN2(6–20)	FKRLEKLFSKIQNDK	+3
HPN3(8–20)	RLEKLFSKIQNDK	+2
HPC1(2–18)	AKKVFKRLEKLFSKIQN	+5
HPC2(2–16)	AKKVFKRLEKLFSKI	+5
HPC3(2–14)	AKKVFKRLEKLFS	+4
HPN1C2(4–16)	KVFKRLEKLFSKI	+4
HPN1C3(4–14)	KVFKRLEKLFS	+3
HPN2C4(6–13)	FKRLEKLF	+2
Amino-acid substitution of HP(2–20)		
HPA1	AKKVFKRLEKLFSKIQN**W**K	+6
HPA2	AKKVFKRLEKLFSKI**W**NDK	+5
HPA3	AKKVFKRLEKLFSKI**W**N**W**K	+6
HPA4	AKKVFKRLEK**S**FSKIQNDK	+5
HPA5	AKKV**S**KRLEKLFSKIQNDK	+5
HPA3A1	**W**KKVFKRLEKLFSKI**W**N**W**K	+6
Truncation and amino-acid substitution of HPA3		
HPA3NT0	FKRLEKLFSKIWNWK	+4
HPA3NT1	FKRL**K**KLFSKIWNWK	+6
HPA3NT2	FKRLEKLF**K**KIWNWK	+5
HPA3NT3	FKRL**K**KLF**K**KIWNWK	+7
Amino-acid substitution of HPC2		
HPC2A3	AKKVFKRL**R**KLF**K**KI	+8
Control peptide		
Melittin	GIGAVLKVLTTGLPALISWIKRKRQQ	+5

Each peptide sequence is labeled with a serial number on the left and the sample name on the right. Amino acid substitutions are indicated in bold letters.

mised individuals. The MICs of the peptides toward *C. albicans* are shown in Table 2. The data revealed that the peptides except some peptide, including the parental HP(2–20), were active in low-salt buffer (buffer I), and that the more hydrophobic analogues HPA3, HPA3A1 and HPA3NT3 showed far more profound activity against yeast than did HP(2–20).

HPA3, HPA3A1, and HPA3NT3 also showed profound antimicrobial activity against Gram-positive (*S. aureus*) and Gram-negative (*E. coli*) bacteria (Table 2), with MICs even lower than those observed with *C. albicans*. This probably reflects the fact that the bacterial membrane is more highly negatively charged than is the zwitterionic yeast membrane. We also tested the peptides via a hemolytic assay, using a highly diluted (8%) hRBC suspension. Peptide hydrophobicity augmented the hemolytic activity of the analogues, but with the exception of HPA3A1, the peptides showed little or no hemolytic activity at their MICs (Table 2). Potential lytic effects were assessed via MTT assays in the culture media of peptide-treated cells. The cell viability assay of the peptides designed in this study against HaCaT cell lines was determined via MTT assay. All tested peptides with the exception of HPA3A1 showed little or no cytotoxic activity (Table 2). This suggests that HPA3 and HPA3NT3 peptides represent good candidates for the development of novel antibiotic agents.

3.3. Antimicrobial peptides recognize chitin, peptidoglycan and LPS in cell wall

We then assessed the capacity of HP(2–20) and melittin to bind to various cell wall components, and determined that all of them bound specifically to chitin and peptidoglycan, but not to chitosan, cellulose, or β-1,3-glucan (Fig. 1A and B). Thus, the potency of a peptide's antimicrobial activity appears to be associated with its binding affinity to chitin and peptidoglycan. Consistent with that notion, the MICs of the peptides toward microbial cells were similar to their binding affinities (Fig. 1C), such that the highly active peptides, HPA3, HPA3NT3, and melittin bound potently to chitin and peptidoglycan in both buffer I and II and LPS in buffer I. In contrast, HPN3, HPN2C4, HPA4, and HPA5 were practically inactive and showed no binding to these cell wall components. We also compared the *in vivo* effects of the peptides on *Aspergillus flavus* and *Aspergillus fumigatus*, two fungi that do express chitin, and on *Phytophthora nicotinae* and *Phytophthora parasitica*, two fungi that do not express chitin (Table 3). We determined that HPA3, HPA3NT3, and melittin showed highly potent antimicrobial activity against the chitin-harboring fungi, but were inactive against strains that did not harbor chitin. The other tested peptides showed no antifungal activity.

3.4. Binding and permeabilization on various lipids

We utilized various lipids to determine the effects of the antimicrobial peptides on the plasma membranes of bacteria [30] and RBCs [31]. One feature that distinguishes the membranes of prokaryotic organisms from those of eukaryotic organisms is that only the former harbor negatively charged lipids in the outer leaflet of the plasma membrane [32]. We discovered that the peptides associated readily with the PG and CL lipid possessing negative charge in the bacterial membrane components (Fig. 2).

Table 2
Antimicrobial and hemolytic activities of HP(2–20) and its analogues

Peptide designation	MICs of peptide (μM)						Hemolysis[a] (%)	Cytotoxicity[b] (%)
	C. albicans		*S. aureus*		*E. coli*			
	Buffer I	Buffer II	Buffer I	Buffer II	Buffer I	Buffer II		
HP	25	>200	6.25	>100	6.25	12.5	0	0
HPN1	100	>200	6.25	>100	6.25	50	0	0
HPN2	>100	>200	100	>100	25	>100	0	0
HPN3	>100	>200	>100	>100	>100	>100	0	0
HPC1	25	>200	6.25	>100	6.25	12.5	0	0
HPC2	25	200	3.12	100	3.12	6.25	0	0
HPC3	50	>200	6.25	>100	6.25	>100	0	0
HPN1C2	50	>200	6.25	>100	6.25	100	0	0
HPN1C3	100	>200	25	>100	6.25	>100	0	0
HPN2C4	>100	>200	>100	>100	>100	>100	0	3.24
HPA1	25	100	3.12	25	3.12	12.5	0	0
HPA2	25	100	3.12	25	3.12	12.5	0	0
HPA3	6.25	25	0.78	6.25	1.56	3.12	23.11	15.14
HPA4	100	>200	25	>100	6.25	100	0	4.12
HPA5	>100	>200	50	>100	6.25	100	0	3.25
HPA3A1	6.25	25	0.78	3.12	3.12	6.25	94.69	100
HPA3NT0	25	100	6.25	50	6.25	12.5	4.70	0
HPA3NT1	25	50	3.12	25	3.12	6.25	9.65	0
HPA3NT2	25	50	1.56	12.5	3.12	6.25	14.92	11.38
HPA3NT3	12.5	12.5	0.78	3.12	0.78	3.12	11.62	8.76
HPC2A3	12.5	100	3.12	100	3.12	6.25	4.5	13.20
Melittin	3.12	6.25	0.78	1.56	0.78	0.78	100	100

[a] Hemolysis percentage at 100 μM of peptide in buffer II.
[b] Cytotoxicity at 25 μM of peptides.

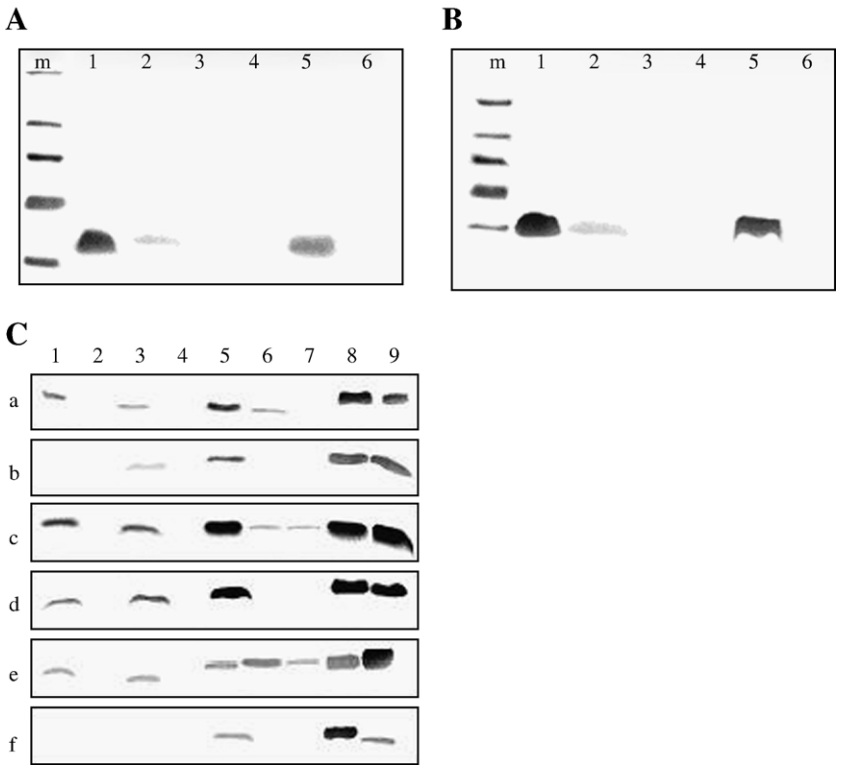

Fig. 1. Binding activity of the synthetic peptides. *In vitro* binding assays were conducted using various cell wall components (A, B and C). The assayed peptides were HP(2–20) (A) and melittin (B): lane 1, control; lane 2, chitin; lane 3, chitosan; lane 4, cellulose; lane 5, peptidoglycan; lane 6, β-1,3-glycan. (C) Binding of synthetic peptides to chitin and peptidoglycan. The assay was conducted as in panels A and B, except that 10-μg samples of peptide were employed: a–d, Binding to chitin (a, b) and peptidoglycan (c, d) in buffer I (a, c) and buffer II (b, d), respectively. e and f were performed against LPS with buffer I and buffer II. The assayed peptides were HP (2–20) (lane 1), HPN3 (lane 2), HPC2 (lane 3), HPN2C4 (lane 4), HPA3 (lane 5), HPA4 (lane 6), HPA5 (lane 7), HPA3NT3(lane 8) and melittin (lane 9).

Thus, the selective antibacterial activity of peptides is probably exerted at the level of the charge on the anionic membrane surface of these microorganisms. Distinctively, although the HPA3NT3 had a strong antibacterial activity, it did not strongly bind to PG.

The capacity of the peptides to permeabilize membranes was assessed via measurements of the release of the fluorescent marker calcein from liposomes with different lipid compositions (Fig. 3). The activities of HPA3, HPA3NT3, and melittin were most pronounced against liposomes composed of zwitterionic PC, indicating an almost total disruption of these vesicles at a concentration of 4 μM. At the same concentration, HP(2–20) and HPN3 released 42% and 16% of the total entrapped calcein respectively. In addition, sphingomyelin exerted an appreciable effect on the permeabilizing activity of HPA3, HPA3NT3, and melittin, which suggests that the cytotoxic activity of peptides against RBCs is associated with the level of their hydrophobicity. However, we detected substantial differences in the permeabilizing ability of the peptides against liposomes comprised of cardiolipin (diphosphatidyl glycerol), a unique four-tailed, doubly negatively-charged lipid phosphoglyceride which is detected predominantly within the fungal plasma membrane, and is believed to be a key determinant of

Table 3
Antifungal activity against fungi with cell wall that do or do not contain chitin

Fungi	MIC (μM)			
	HP(2–20)	HPA3	HPA3NT3	Melittin
Aspergillus flavus	25	6	4	6
Aspergillus fumigatus	25	6	4	6
Phytophthora nicotinae	>100	>100	>100	>100
Phytophthora parasitica	>100	>100	>100	>100

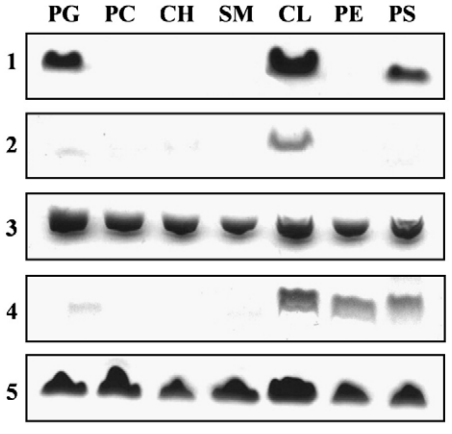

Fig. 2. Binding assay of the synthetic peptides. *In vitro* binding assays were conducted using various cell membrane components. Interaction between synthetic peptides and liposomes composed of the indicated lipids were assayed. 1, HP(2–20); 2, HPN3; 3, HPA3; 4, HPA3NT3; 5, melittin.

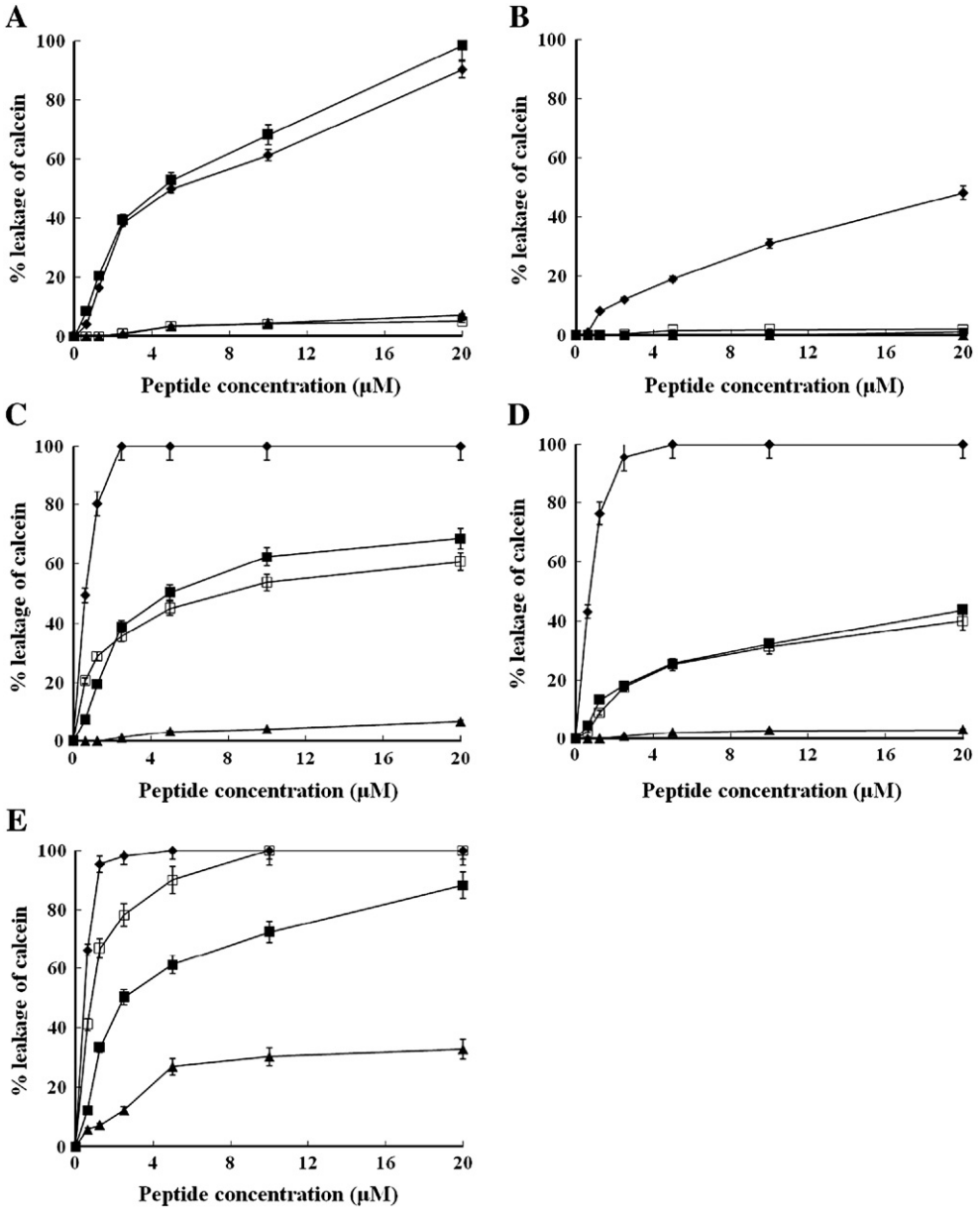

Fig. 3. Peptide-induced release of calcein from liposomes. Calcein-containing liposomes composed of the indicated lipids were prepared and quantified as described in Materials and methods. Liposome suspensions containing 100 μM lipids (◆:PC, ■: PG, ▲: CL, and □: SM) were incubated with HP(2–20) (A), HPN3 (B), HPA3 (C), HPA3NT3 (D), and melittin (E). The fluorescence of the released calcein was then assessed using a spectrofluorometer (excitation, 480 nm; emission, 520 nm). 100% release was achieved using 1 mM Triton X-100.

fungal cell membrane potential and permeability. We determined that melittin released approximately 32.69% of total calcein at a concentration of 20 μM, whereas HPA3 and HPA3NT3 exerted very little effect, which is consistent with their respective activities against *C. albicans* (Table 2).

3.5. Peptide-induced membrane depolarization in bacteria, bacterial spheroplasts, and yeast

In order to further determine the manner in which the interaction of these peptides with the bacterial plasma membrane results in cell death, we evaluated the ability of the peptides to induce membrane depolarization in both bacteria and bacterial spheroplasts (LPS and peptidoglycan-free bacteria). The peptides were added to *S. aureus* ATCC 25923 (Fig. 4A), spheroplasts of *E. coli* ATCC 25922 (Fig. 4B), intact *E. coli* ATCC 25922 (Fig. 4C) or *C. albicans* (Fig. 4D) under conditions similar to those previously reported [28]. Fig. 4 shows the dose-dependent dissipation of the membrane potential by peptides, which reveals there to be a direct correlation between the peptide's antimicrobial activity and its ability to dissipate the bacterial membrane potential. This suggests that the main target of these peptides is the bacterial cytoplasmic membrane (inner membrane). Of note is that once the cell wall (outer membrane) is removed, HPA3, HPA3NT3 and melittin potently affect membrane potential. In addition, HPA3 and HPA3NT3 showed a

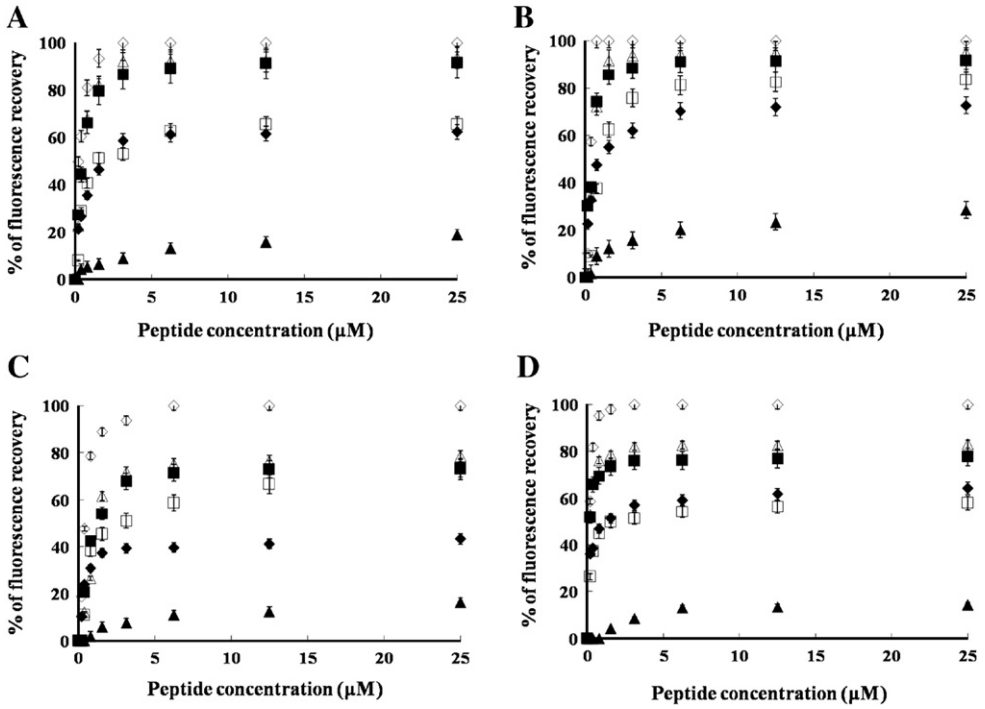

Fig. 4. Peptide-induced depolarization of bacterial and fungal membranes (A, B, C and D). The indicated peptides were added to *S. aureus* (A), spheroplasts of *E. coli* ATCC 25922 (B), intact *E. coli* ATCC 25922 (C), or *C. albicans* (D) that had been pre-equilibrated for 60 min with diS-C_3-5. Fluorescence recovery was measured 1–120 min (at 5-min intervals) after the peptides (◆, HP(2–20); ■, HPA3; ▲, HPN3; △, HPA3NT3; □, HPC2A3; ◇, melittin) had been mixed with the bacteria. Shown are the maximum fluorescences.

greater ability to induce membrane depolarization in intact *C. albicans* than the other analogues, which is consistent with their greater ability to induce calcein release.

3.6. The sizes of the different pores formed between peptides

In order to gather additional clues as to the type and extent of membrane damage induced by HP(2–20) and its analogues, we assessed the peptide-induced release of fluorescently labeled dextran molecules of various sizes – i.e., FD4 (3.9 kDa, 1.8 nm radii), FD10 (9.9 kDa), FD20 (19.8 kDa, 3.3 nm radii), FD40 (40.5 kDa, 4.8 nm radii), FD70 (71.6 kDa, 5 nm radii) and FD500 (530 kDa). FD-entrapped liposomes were incubated with 10 μM of the peptides (peptide/lipid ratio = 1/10) [33–35]. Assessing the differences in the sizes of the pores formed, one may distinguish between peptides that function in a barrel-stave manner or in a toroidal manner [36]. We determined that the evoked release of FD varied inversely with its molecular mass/size (Fig. 5A–D). For instance, HPA3, HPA3NT3 and melittin released 100% of the FD4 from PC liposomes, but only 52% of FD70. HP(2–20) released only 33% of the FD4 from PC vesicles, and was unable to release any of the larger markers. The pore created by HP(2–20) indicates that the radius is approximately 1.8 nm and pores induced by HPA3, HPA3NT3 and melittin have apparent radii between 3.3 and 4.8 nm at a 1/10 (peptide/lipid) molar ratio concentration.

When we compared the extents of release from liposomes comprised of PC/cholesterol (Fig. 5B) or PE/PG (Fig. 5C), we determined that release from the former was peptide-specific, whereas release from the latter did not vary among the peptides. Finally, using liposomes composed of PC/cholesterol/sphingomyelin (hRBC, 1:1:1, w/w/w), we determined that the introduction of Trp into peptides (HPA3, HPA3NT3 and melittin) resulted in a dramatic increase in the extent of release, which is consistent with the observed hemolytic activities of those peptides (Table 2 and Fig. 5D).

3.7. HPA3, HPA3NT3 and Melittin oligomers generate ring-like structures in transmission electron microscopy

In order to characterize the oligomeric states of the membrane-bound peptides, we conducted chemical crosslinking in the presence of liposomes. When bound to liposomes composed of PC/cholesterol (1:1, w/w), HP(2–20) assumed a uniquely dimeric form, whereas HPA3 formed more multimeric complexes (~8 mer, Fig. 6C).

We next employed transmission electron microscopy in order to directly observe the formation of the peptide-induced pores. In these experiments, liposome composed of PC/cholesterol or PE/PG was incubated for 5 min with the indicated peptides. Fig. 6A shows that HPA3, HPA3NT3, and melittin form ring-like structures on the vesicles, which can be either attached to the vesicle or released into the solution (panels 3–5). The pores consisted of 7-to 8-nm-wide rings which encircled 3.5-to 4.5-nm-wide cavities, and were formed by complexes (~8 mer) of HPA3, HPA3NT3, or melittin bound to the membranes. These results were consistent with those of the FD-leakage assay and cross-linking data in liposomes (Fig. 6C).

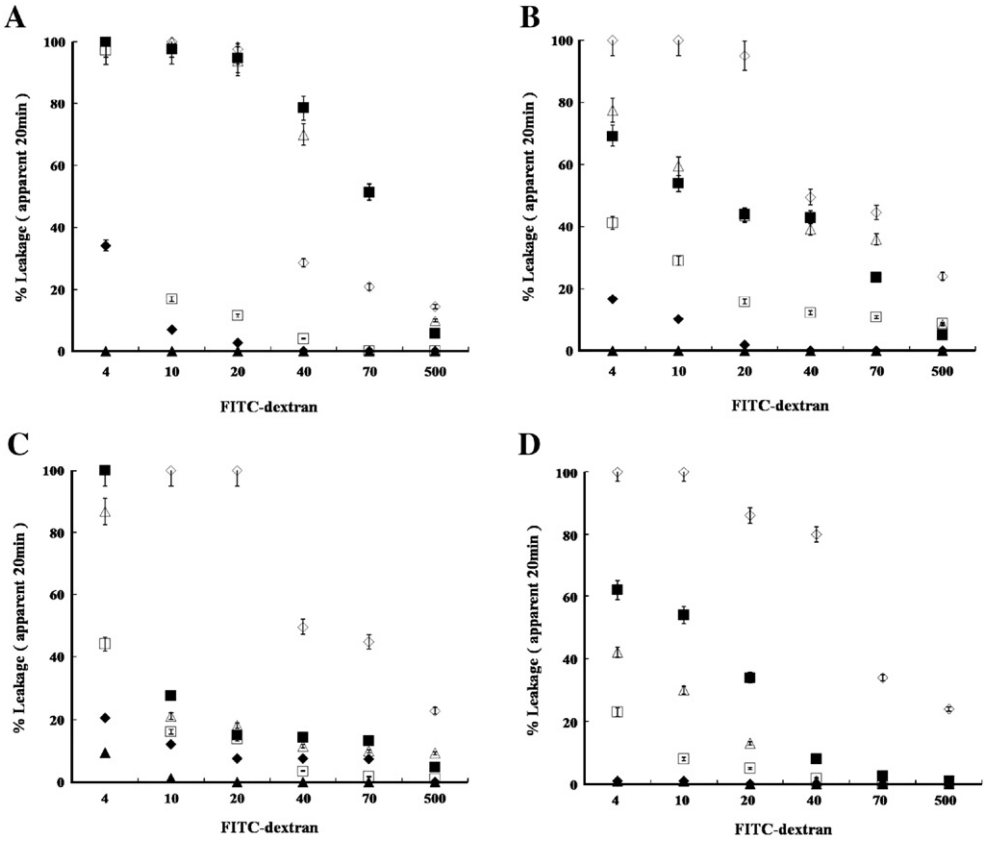

Fig. 5. The lipid compositions (A, PC; B, PC/CH (1:1); C, PE/PG (1:1); D, PC/CH/SM (1:1:1)) of the liposomes containing FD4, 10, 20, 40, 70, or 500 are indicated in the text; they were prepared and quantified as described in Materials and methods. The release of dextran was fluorometrically determined. The apparent percentage of release was calculated as $100\times(F-F_0)/(F_t-F_0)$, in which F and F_t are the fluorescence intensities prior to and after the addition of the peptide (◆ HP(2–20); ▲, HPN3; ■, HPA3; △, HPA3NT3; □, HPC2A3; ◇, melittin), respectively, and F_0 is the fluorescence of the intact vesicles. Values are expressed as an average of three independent measurements.

3.8. The effects of peptides on the morphology of cells were observed using scanning electron microscopy

The effects of HP(2–20), HPA3, and HPA3NT3 on the morphology of *E. coli, S. aureus* and *C. albicans* were determined via scanning electron microscopy. When the peptides were applied at concentrations corresponding to an MIC of 60%, some differences were observed in the morphology of the treated bacteria. HP(2–20) induced flabbiness over the complete cell wall (Fig. 7A–C, panel 2), whereas HPA3, HPA3NT3, and melittin induced local perturbations and blebs (Fig. 7A–C, panels 3–5). This difference may reflect the fact that HP(2–20) reaches the membrane predominantly in the form of monomers that aggregate on the surfaces of negatively-charged membranes once a threshold concentration has been reached [33], whereas HPA3, HPA3NT3, and melittin reach the membrane as highly-ordered oligomers.

3.9. Structural analysis of peptides were observed using CD Measurements in membrane mimicking environment

In order to investigate the relationship of the structure and the antibiotic activity of the peptides on lipids, the CD spectra of the peptides in phosphate buffer, SDS solution or PC/CH liposome was measured. All peptides showed a random coil structure in an aqueous solution, while displaying a typical α-helical spectrum with two minimum peaks at 208 and 222 nm in 30 mM SDS or PC/CH liposome solution (Fig. 8). HP(2–20), HPA3, HPA3NT3 formed α-helical structures except HPN3 in 30 mM SDS or PC/CH liposome solution. HPA3 and HPA3NT3 have more potent antibiotic activity in bacterial and fungal cells than HP (2–20), while displaying higher α-helicity than HP (2–20) in liposome (Fig. 8). These results suggest that the α-helical content in liposome may be correlated with the enhanced antibiotic activity in killing bacterial and fungal cells.

4. Discussion

Linear antimicrobial peptides that assume an amphipathic α-helical structure upon binding to bacterial membranes are among the most abundant and widespread in nature. The majority of cationic antimicrobial peptides possess bacteria cell-selective activity, binding specifically to negatively-charged phospholipids, which are the principal components of bacterial cytoplasmic membranes [37,38], then permeabilizing the membrane. They have substantially less affinity for zwitterionic membranes, which mimic the membranes of fungi and other eukaryotic cells. In our earlier study, we attempted to obtain

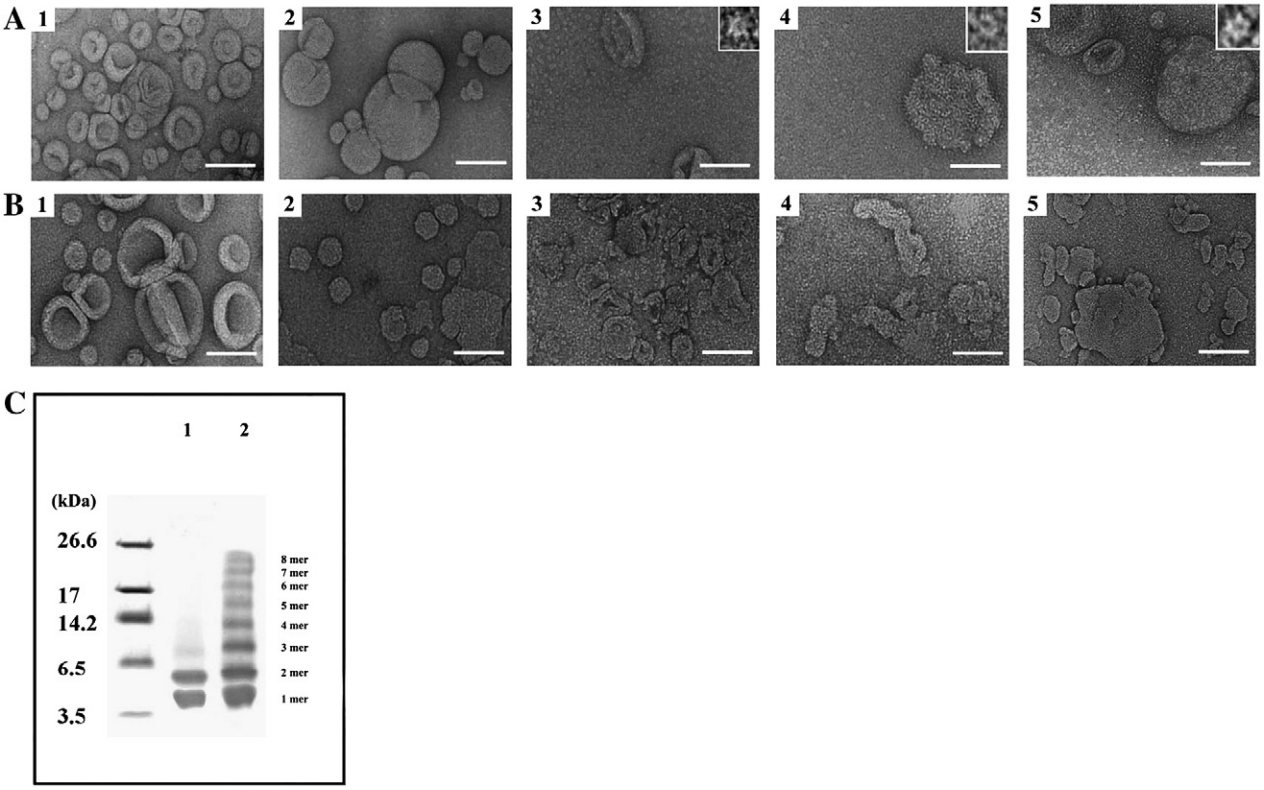

Fig. 6. Electron micrographs and cross-linking. Transmission electron micrographs showing the morphological changes in liposomes composed of PC/cholesterol (1:1) (A) and PE/PG (1:1) (B). (A) Electron micrographs of PC/cholesterol liposomes in the absence (1) and presence of HP(2–20) (2), HPA3 (3), HPA3NT3 (4) or Melittin (5). (B) Electron micrographs of PE/PG liposomes incubated with the same tested peptides. The insets show a highly ordered pore. Scale bar indicates 100 nm. (C) The chemical cross-linking of peptides bound to liposomes composed of PC/CH (1:1, w/w): lane M, Marker; lane 1, HP(2–20); lane 2, HPA3.

peptides that augmented antibiotic activity but showed little or no cytotoxicity, and therefore designed novel peptide analogues of HP(2–20) via the substitution of amino acids on the basis of the peptide sequence and the effect on the α-helical wheel diagram [39]. Such substitutions can alter the tertiary structure of the HP(2–20) peptide, and may also confer potent antibiotic activity [40].

In the present study, peptide sequences were altered using four types of modification: (i) To determine the influence of changes in the N- or C-terminal amino acids, and thus the

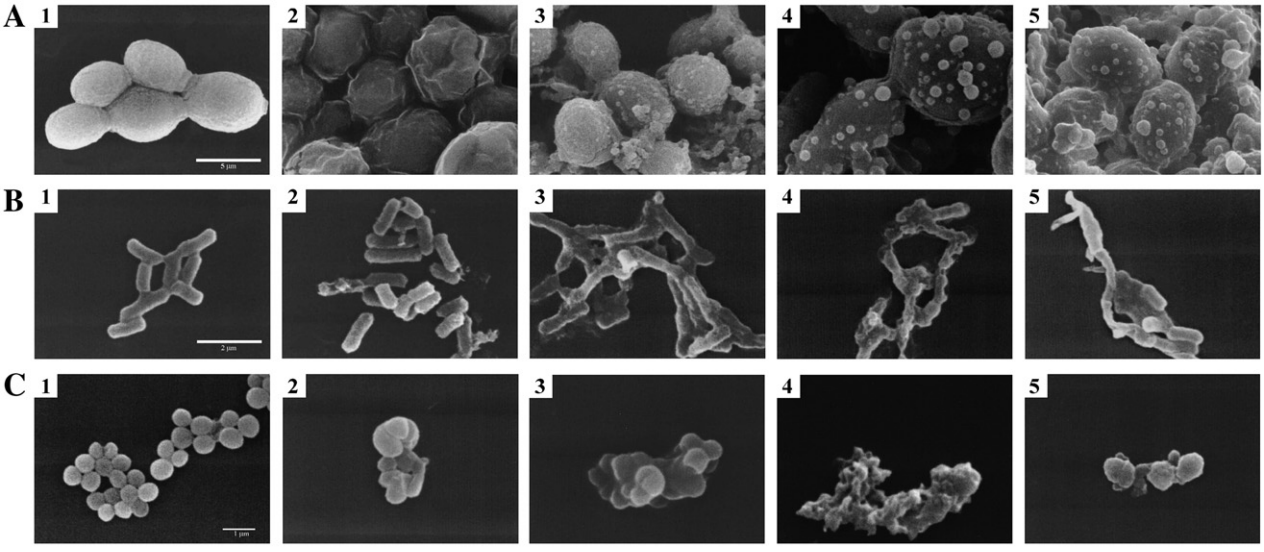

Fig. 7. Scanning electron micrographs of *C. albicans* (A), *E. coli* (B), and *S. aureus* (C) exposed to the indicated peptides at 60% MIC: panel 1, untreated peptide; panel 2, HP(2–20); panel 3, HPA3; panel 4, HPA3NT3; panel 5, melittin.

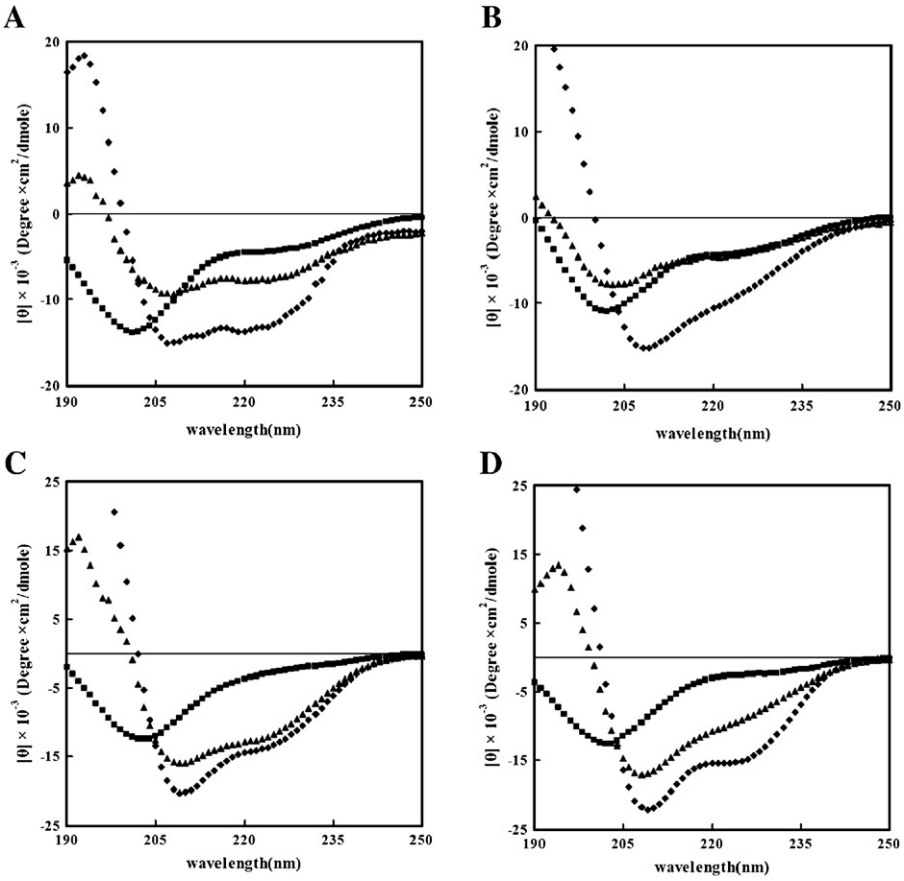

Fig. 8. CD spectra of HP (2–20) (A), HPN3 (B), HPA3 (C) and HPNT3 (D) in aqueous solution (■), 30 mM SDS micelles (▲) and 1 mM PC/CH liposome (♦). The concentration of peptides was 50 μM. CD spectra were recorded at 25 °C on a Jasco 810 spectropolarimeter (Jasco, MD, USA) equipped with a temperature control unit. A 0.1-cm path-length quartz cell was used for CD analysis. At least five scans were averaged for each sample and the averaged blank spectra were subtracted.

amphipathicity of the peptide, on the antimicrobial activity, we synthesized several peptides truncated from either the N- or C-terminus. Antimicrobial activity against bacterial and fungal cells was substantially attenuated via the removal of the N-terminal amino acid residues of HP(2–20), which diminished the amphipathicity of the peptide (Table 1 and 2) [41]. (ii) Amino acids were substituted without altering the amphipathic organization. The augmentation of the hydrophobicity of the peptides via the substitution of Trp for Gln and Asp at positions 17 and 19 of HP(2–20) (HPA3) induced a dramatic increase in selective antibacterial and antifungal activity, which suggests that this peptide may facilitate not only the understanding of the mechanism of action of the α-helical antibiotic peptides, but also the design of novel antibiotics with enhanced antibiotic activity. Interestingly, the substitution of Trp for all of the hydrophobic amino acids – i.e., Ala, Gln and Asp at positions 2, 17 and 19 (HPA3A1) – increased the antimicrobial activity of HP(2–20), but this analogue was also potently hemolytic and cytotoxic (Table 2). Apparently, the tryptophan residue is a key determinant of the hemolytic and cytotoxic properties of the peptide. (iii) The addition of positive charges to the peptide via the substitution of Lys for Ser and/or Glu (HPA3NT0-3) did not significantly affect the peptides' potency or spectrum of activity, but did make it increasingly less hemolytic and cytotoxic. (iv) Deletion of the C-terminal and the addition of the positively-charged Arg and Lys (HPC2A3) effected an increase in the antimicrobial activity of HPC2, although it remained less potent than that of HPA3.

We also determined that HP(2–20) and its analogues specifically recognize common immune elicitors, including chitin, peptidoglycan, and LPS (Table 3 and Fig. 1A–C). Antimicrobial peptides must first be attracted to bacterial or fungal surfaces, and one obvious mechanism by which this may occur involves electrostatic bonding between anionic or cationic peptides and structures on the surface. Previous studies have demonstrated that peptides such as magainin 2 and cecropin A can be readily inserted into monolayers, LUVs, and liposomes harboring acidic phospholipids [42,43]. However, Gram-negative and Gram-positive bacteria are far more complex than model membranes, and cationic antimicrobial peptides are likely to be attracted first to the net negative charge existing on the outer envelope of Gram-negative bacteria – e.g., the anionic phospholipids and phosphate groups on LPS – and to the teichoic acids located on the surface of Gram-positive bacteria. Artificial chimeric peptides, such as CEME-related peptides, bind to both LPS and lipoteichoic acid [44], but this binding is not associated with their ability to kill bacteria, thereby suggesting that peptides use this binding only to come into contact with other targets, including the cytoplasmic membrane.

Similar to many native antimicrobial peptides, HP(2–20) and the majority of its analogues were not hemolytic up to the maximal tested concentrations (200 μM) (Table 2), despite the fact that several of the more hydrophobic analogues also permeate the zwitterionic membranes, although less efficiently than the negatively-charged membranes (Fig. 2). Human RBCs are rich in negatively-charged sialic acid-harboring carbohydrate moieties in the form of glycoproteins and glycosphingolipids, which comprise the glycocalix layer. It is possible that the peptides stick to the negatively-charged glycocalix layer and, due to their limited capacity to partition within the zwitterionic membranes [45], they cannot diffuse into the membrane. There is also a general consensus that hydrophobic peptide–membrane interactions may determine hemolytic potency [46], which is correlated with the relatively high hydrophobicity and hydrophobic moments displayed by more hydrophobic HP(2–20) analogues, including HPA3 and HA3A1. This increase in hydrophobicity may compensate for the lack of amphipathic structure.

The peptides were also evaluated with regard to their ability to dissipate the membrane potential of intact *S. aureus* and *C. albicans,* as well as the spheroplasts of two *E. coli* strains with differing susceptibilities to the tested peptides (Fig. 4). We determined there to be a direct correlation between the MICs of the tested peptides toward *S. aureus* and *C. albicans* and their ability to disrupt membrane potential (Fig. 4A). We determined that all of the peptides showed similar activities toward the spheroplasts (Fig. 4B), which indicates that the cytoplasmic membrane is their target and that the differences in their activities toward intact cells is reflective of their differing abilities to diffuse through the outer membrane. Once across the outer membrane, the peptides evidence similar abilities with regard to the permeation of the cytoplasmic membrane.

We also determined that HP(2–20) and HPA3 strongly interact with neutral zwitterionic lipid bilayers. This interaction results in the perturbation of membrane integrity and the lysis of lipid vesicles, as demonstrated by the release of fluorescent markers (Fig. 5A–D). As was previously reported for temporins A and B [47], the extent of the release was related inversely to the size of the entrapped marker, which is indicative of the formation of pores or local breaks within the membrane, rather than complete membrane disruption via a detergent-like action [48].

In addition, HPA3 reaches the cell membranes in oligomeric form, where it forms toroidal pores, as was observed in the cross-linking experiments (Fig. 6C) and transmission electron micrographs, whereas HP(2–20) does not assume a highly-ordered oligomeric form (Fig. 6A and B). The difference between the morphology of the patches on the bacterial cell wall observed with HPA3, HPA3NT3 and melittin (Fig. 7A–C) may be related with their different oligomerization states upon reaching the membrane.

Although the observations collected thus far do not allow us to unequivocally elucidate the mechanism of action of HP(2–20) and its analogues, the available data do suggest that an appropriate balance of hydrophobic and electrostatic interactions must regulate the interaction of these peptides with lipid membranes in a complex manner, and thus modulate both their target cell selectivity and biological properties. Further studies are in progress to determine the membrane activity of HP(2–20) and its analogues in greater detail.

Acknowledgements

This work was supported by grant from the Ministry of Science and Technology, Korea and the Korea Science and Engineering Foundation through the Research Center for Proteineous Materials (R11-2000-083-00000-0), and from the Korea Foundation for International Cooperation of Science & Technology(KICOS) through a grant provided by the Korean Ministry of Science & Technology(MOST) in 2007 (No. K20713000012-07B0100-01210).

References

[1] L. Yang, T.A. Harroun, T.M. Weiss, L. Ding, H.W. Huang, Barrel-stave model or toroidal model? A case study on melittin pores, Biophys. J. 81 (2001) 1475–1485.
[2] G. Ehrenstein, H. Lecar, Electrically gated ionic channels in lipid bilayers, Q. Rev. Biophys. 10 (1977) 1–34.
[3] P.C. Dave, E. Billington, Y.L. Pan, S.K. Straus, Interaction of alamethicin with ether-linked phospholipid bilayers: oriented circular dichroism 31P solid-state NMR, and differential scanning calorimetry studies, Biophys. J. 89 (2005) 2434–2442.
[4] M.T. Lee, F.Y. Chen, H.W. Huang, Energetics of pore formation induced by membrane active peptides, Biochemistry 43 (2004) 3590–3599.
[5] F.Y. Chen, M.T. Lee, H.W. Huang, Evidence for membrane thinning effect as the mechanism for peptide-induced pore formation, Biophys. J. 84 (2003) 3751–3758.
[6] A. Spaar, C. Munster, T. Salditt, Conformation of peptides in lipid membranes studied by X-ray grazing incidence scattering, Biophys. J. 87 (2004) 396–407.
[7] K. He, S.J. Ludtke, H.W. Huang, D.L. Worcester, Antimicrobial peptide pores in membranes detected by neutron in-plane scattering, Biochemistry 34 (1995) 15614–15618.
[8] K. He, S.J. Ludtke, D.L. Worcester, H.W. Huang, Neutron scattering in the plane of membranes: structure of alamethicin pores, Biophys. J. 70 (1996) 2659–2666.
[9] R.S. Cantor, Size distribution of barrel-stave aggregates of membrane peptides: influence of the bilayer lateral pressure profile, Biophys. J. 82 (2002) 2520–2525.
[10] S. Yamaguchi, D. Huster, A. Waring, R.I. Lehrer, W. Kearney, B.F. Tack, M. Hong, Orientation and dynamics of an antimicrobial peptide in the lipid bilayer by solid-state NMR spectroscopy, Biophys. J. 81 (2001) 2203–2214.
[11] Y. Pouny, D. Rapaport, A. Mor, P. Nicolas, Y. Shai, Interaction of antimicrobial dermaseptin and its fluorescently labeled analogues with phospholipid membranes, Biochemistry 31 (1992) 12416–12423.
[12] B. Bechinger, The structure, dynamics and orientation of antimicrobial peptides in membranes by multidimensional solid-state NMR spectroscopy, Biochim. Biophys. Acta 1462 (1999) 157–183.
[13] Y. Shai, Mechanism of the binding, insertion and destabilization of phospholipid bilayer membranes by alpha-helical antimicrobial and cell non-selective membrane-lytic peptides, Biochim. Biophys. Acta 1462 (1999) 55–70.
[14] A.S. Ladokhin, S.H. White, 'Detergent-like' permeabilization of anionic lipid vesicles by melittin, Biochim. Biophys. Acta 1514 (2001) 253–260.
[15] K. Matsuzaki, O. Murase, N. Fujii, K. Miyajima, An antimicrobial peptide, magainin 2, induced rapid flip-flop of phospholipids coupled with pore formation and peptide translocation, Biochemistry 35 (1996) 11361–11368.
[16] S. Yamaguchi, T. Hong, A. Waring, R.I. Lehrer, M. Hong, Solid-state NMR investigations of peptide–lipid interaction and orientation of a beta-

sheet antimicrobial peptide, protegrin, Biochemistry 41 (2002) 9852–9862.
[17] K. Matsuzaki, K. Sugishita, N. Ishibe, M. Ueha, S. Nakata, K. Miyajima, R.M. Epand, Relationship of membrane curvature to the formation of pores by magainin 2, Biochemistry 37 (1998) 11856–11863.
[18] S.J Ludtke, K. He, W.T. Heller, T.A. Harroun, L. Yang, H.W. Huang, Membrane pores induced by magainin, Biochemistry 35 (1996) 13723–13728.
[19] L. Yang, T.M. Weiss, P.I. Lehrer, H.W. Huang, Crystallization of antimicrobial pores in membranes: magainin and protegrin, Biophys. J. 79 (2000) 2002–2009.
[20] N. Papo, Y. Shai, Exploring peptide membrane interaction using surface plasmon resonance: differentiation between pore formation versus membrane disruption by lytic peptides, Biochemistry 42 (2003) 458–466.
[21] K. Matsuzaki, K. Sugishita, M. Harada, N. Fujii, K. Miyajima, Interactions of an antimicrobial peptide, magainin 2, with outer and inner membranes of Gram-negative bacteria, Biochim. Biophys. Acta 1327 (1997) 119–130.
[22] L.A. Allen, Modulating phagocyte activation: the pros and cons of *Helicobacter pylori* virulence factors, J. Exp. Med. 191 (2000) 1451–1454.
[23] K. Pütsep, C.I. Bränden, H.G. Boman, S. Normark, Antibacterial peptide from *H. pylori*, Nature 398 (1999) 671–672.
[24] J. Bylund, T. Christophe, F. Boulay, T. Nyström, A. Karlsson, C. Dahlgren, Proinflammatory activity of a cecropin-like antibacterial peptide from *Helicobacter pylori*, Antimicrob. Agents Chemother. 45 (2001) 1700–1704.
[25] A. Makino, T. Baba, K. Fujimoto, K. Iwamoto, Y. Yano, N. Terada, S. Ohno, S.B. Sato, A. Ohta, M. Umeda, K. Matsuzaki, T. Kobayashi, J. Biol. Chem. 278 (2003) 3204–3209.
[26] K. Matsuzaki, K. Sugishita, K. Miyajima, Interactions of an antimicrobial peptide, magainin 2, with lipopolysaccharide-containing liposomes as a model for outer membranes of Gram-negative bacteria, FEBS Lett. 449 (1999) 221–224.
[27] O.S. Belokoneva, H. Satake, E.L. Mal'tseva, N.P. Pal'mina, E. Villegas, T. Nakajima, G. Corzo, Pore formation of phospholipid membranes by the action of two hemolytic arachnid peptides of different size, Biochim. Biophys. Acta 1664 (2004) 182–188.
[28] J.C.M. Stewart, Colorimetric determination of phospholipids with ammonium ferrothiocyanate, Anal. Biochem. 104 (1980) 10–14.
[29] C. Maeng, M.S. Oh, I.H. Park, H.J. Hong, Purification and structural analysis of the hepatitis B virus preS1 expressed from *Escherichia coli*, Biochem. Biophys. Res. Commun. 282 (2001) 787–792.
[30] J.A. Op den Kamp, Lipid asymmetry in membranes, Ann. Rev. Biochem. 48 (1979) 47–71.
[31] M.A. Yorek, Phospholipids Handbook, Marcel Dekker, New York, 1993.
[32] M. Wu, E. Maier, R. Benz, R.E. Hancock, Mechanism of interaction of different classes of cationic antimicrobial peptides with planar bilayers and with the cytoplasmic membrane of *Escherichia coli*, Biochemistry 38 (1999) 7235–7242.
[33] A.S. Ladokhin, M.E. Selsted, S.H. White, Sizing membrane pores in lipid vesicles by leakage of co-encapsulated markers: pore formation by melittin, Biophys. J. 72 (1997) 1762–1766.
[34] M.P. Bohrer, W.M. Deen, C.R. Robertson, J.L. Troy, B.M. Brenner, Influence of molecular configuration on the passage of macromolecules across the glomerular capillary wall, J. Gen. Physiol. 74 (1979) 583–593.
[35] F. Szoka Jr., D. Papahadjopoulos, Procedure for preparation of liposomes with large internal aqueous space and high capture by reverse-phase evaporation, Proc. Natl. Acad. Sci. U. S. A. 75 (1978) 4194–4198.
[36] E. Gazit, W.J. Lee, P.T. Brey, Y. Shai, Mode of action of the antibacterial cecropin B2: a spectrofluorometric study, Biochemistry 33 (1994) 10681–10692.
[37] Y. Shai, From innate immunity to de-novo designed antimicrobial peptides, Curr. Pharm. Des. 8 (2002) 715–725.
[38] R.E. Hancock, A. Rozek, Role of membranes in the activities of antimicrobial cationic peptides, FEMS Microbiol. Lett. 206 (2002) 143–149.
[39] D.G. Lee, H.N. Kim, Y. Park, H.K. Kim, B.H. Choi, C.H. Choi, K.-S. Hahm, Design of novel analogue peptides with potent antibiotic activity without hemolytic activity based on the antimicrobial peptide derived from N-terminal sequence of *Helicobacter pylori* Ribosomal Protein L1, Biochim. Biophys. Acta 1598 (2002) 185–194.
[40] K.H. Lee, D.G. Lee, Y. Park, D.I. Kang, S.Y. Shin, K.–S. Hahm, Y. Kim, Interactions between the antimicrobial peptide, HP (2–20) and its analogues derived from *Helicobacter pylori,* and membrane, Biochem. J. 394 (2006) 105–114.
[41] Y. Park, D.G. Lee, H.N. Kim, K.K. Kim, E.-R. Woo, C.H. Choi, K.-S. Hahm, Importance of the length of the *N*- and *C*-terminal regions of *Helicobacter pylori* ribosomal protein L1 (RPL1) on antimicrobial activity, Biotechnol. Lett. 24 (2002) 1209–1215.
[42] K. Matsuzaki, M. Harada, S. Funakoshi, N. Fujii, K. Miyajima, Physicochemical determinants for the interactions of magainins 1 and 2 with acidic lipid bilayers, Biochem. Biophys. Acta 1963 (1991) 162–170.
[43] B. Christensen, J. Fink, R.B. Merrifield, D. Mauzerall, Channel-forming properties of cecropins and related model compounds incorporated into planar lipid membranes, Proc. Natl. Acad. Sci. U. S. A. 85 (1988) 5072–5076.
[44] M.G. Scott, H. Yan, R.E. Hancock, Biological properties of structurally related α-helical cationic antimicrobial peptides, Infect. Immun. 67 (1999) 2005–2009.
[45] K. Matsuzaki, K. Suqishita, N. Fujii, K. Miyajima, Molecular basis for membrane selectivity of an antimicrobial peptide, magainin 2, Biochemistry 34 (1995) 3423–3429.
[46] M. Dathe, M. Schűmann, T. Wieprecht, A. Winkler, K. Matsuzaki, O. Murase, M. Beyermann, E. Krause, M. Bienert, Biochemistry 35 (1996) 12612–12622.
[47] A.C. Rinaldi, A. Di Giulio, M. Liberi, G. Gualtieri, A. Oratore, M.E. Schininá, M. Simmaco, A. Bozzi, Effects of temporins on molecular dynamics and membrane permeabilization in lipid vesicles, J. Pept. Res. 58 (2001) 213–220.
[48] A.S. Ladokhin, M.E. Selsted, S.H. White, Sizing membrane pores in lipid vesicles by leakage of co-encapsulated markers: pore formation by melittin, Biophys. J. 72 (1997) 1762–1766.